Mutational analysis of caveolin-induced vesicle formation

Expression of caveolin-1 recruits caveolin-2 to caveolae membranes

Shengwen Li[1,a], Ferruccio Galbiati[a], Daniela Volonte'[a], Massimo Sargiacomo[b], Jeffrey A. Engelman[a], Kallol Das[c], Philipp E. Scherer[c], Michael P. Lisanti[a,*]

[a]*Department of Molecular Pharmacology, Albert Einstein College of Medicine, 1300 Morris Park Avenue, Bronx, NY 10461, USA*
[b]*Department of Hematology and Oncology, Instituto Superiore di Sanità, Viale Regina Elena 299, 00161 Rome, Italy*
[c]*Department of Cell Biology, Albert Einstein College of Medicine, 1300 Morris Park Avenue, Bronx, NY 10461, USA*

Received 27 May 1998; revised version received 17 July 1998

Abstract **Caveolae are vesicular organelles with a characteristic uniform diameter in the range of 50–100 nm. Although recombinant expression of caveolin-1 is sufficient to drive caveolae formation, it remains unknown what controls the uniform diameter of these organelles. One hypothesis is that specific caveolin-caveolin interactions regulate the size of caveolae, as caveolin-1 undergoes two stages of self-oligomerization. To test this hypothesis directly, we have created two caveolin-1 deletion mutants that lack regions of caveolin-1 that are involved in directing the self-assembly of caveolin-1 oligomers. More specifically, Cav-1 Δ61–100 lacks a region of the N-terminal domain that directs the formation of high molecular mass caveolin-1 homo-oligomers, while Cav-1 ΔC lacks a complete C-terminal domain that is required to allow caveolin homo-oligomers to interact with each other, forming a caveolin network. It is important to note that these two mutants retain an intact transmembrane domain. Our current results show that although Cav-1 Δ61–100 and Cav-1 ΔC are competent to drive vesicle formation, these vesicles vary widely in their size and shape with diameters up to 500–1000 nm. In addition, caveolin-induced vesicle formation appears to be isoform-specific. Recombinant expression of caveolin-2 under the same conditions failed to drive the formation of vesicles, while caveolin-3 expression yielded caveolae-sized vesicles. These results are consistent with the previous observation that in transformed NIH 3T3 cells that lack caveolin-1 expression, but continue to express caveolin-2, no morphologically distinguishable caveolae are observed. In addition, as caveolin-2 alone exists mainly as a monomer or homo-dimer, while caveolins 1 and 3 exist as high molecular mass homo-oligomers, our results are consistent with the idea that the formation of high molecular mass oligomers of caveolin are required to regulate the formation of uniform caveolae-sized vesicles. In direct support of this notion, regulated induction of caveolin-1 expression in transformed NIH 3T3 cells was sufficient to recruit caveolin-2 to caveolae membranes. The ability of caveolin-1 to recruit caveolin-2 most likely occurs through a direct interaction between caveolins 1 and 2, as caveolins 1 and 2 are normally co-expressed and interact with each other to form high molecular mass hetero-oligomers containing both caveolins 1 and 2.**

Key words: Caveolin; Vesicle formation; Caveolae

1. Introduction

Caveolae are 50–100 nm vesicular invaginations of the plasma membrane [1]. They represent a sub-compartment of the plasma membrane. It has been proposed that caveolae participate in vesicular trafficking events and signal transduction processes. Caveolae are most abundant in terminally differentiated cells, such as adipocytes, endothelial cells and muscle cells [2–7].

The specialized lipid composition of caveolae is thought to convey resistance of this membrane domain to detergent solubilization by Triton X-100 (at low temperatures) [3,8–13]. This property appears to be unique to caveolae membranes. For example, when intact cells were fixed in paraformaldehyde and extracted with Triton X-100 and then examined by electron microscopy, the insoluble membranes that remained were found to be caveolae [14].

Caveolin, a 21–24 kDa integral membrane protein, is a principal component of caveolae membranes in vivo. [15–19]. Caveolin is only the first member of a new gene family; as a consequence, caveolin has been re-termed caveolin-1 [4]. Molecular cloning has identified three distinct caveolin genes: caveolin-1, caveolin-2, and caveolin-3. The two isoforms of caveolin-1 (Cav-1α and Cav-1β) are derived from alternative initiation during translation. Caveolins 1 and 2 are most abundantly expressed in adipocytes, endothelial cells and fibroblastic cell types, while the expression of caveolin-3 is muscle-specific [20–23].

Caveolin proteins interact with themselves to form homo- and hetero-oligomers [24,25] which directly bind cholesterol [26], and require cholesterol for insertion into model lipid membranes [26,27]. These caveolin oligomers may also interact with glycosphingolipids, although the evidence is more indirect via chemical cross-linking studies [28]. These protein-protein and protein-lipid interactions are thought to be the driving force for caveolae formation.

Endogenous caveolin-1 is insoluble in non-ionic detergents such as Triton X-100 at low temperatures [8,9]; however, it can be efficiently solubilized by the mild detergent, octyl-glucoside [8,9]. It is thought that octyl-glucoside solubilization occurs through the displacement of endogenous lipid components (such as glycosphingolipids and cholesterol) that are concentrated within caveolae membranes and interact directly with caveolin [3,8–13].

Caveolin-1 is a 22–24 kDa integral membrane protein which consists of 178 amino acid residues. Caveolin-1 assumes an unusual topology. A central hydrophobic domain (residues 102–134) is thought to form a hairpin-like structure within the

*Corresponding author. Fax: (1) (718) 430-8830.
E-mail: lisanti@aecom.yu.edu

[1]Present address: Department of Cell Biology, Harvard Medical School, Boston, MA 02115, USA.

PII: S0014-5793(98)00945-4

membrane (reviewed in [29,30]). As a consequence, both the N-terminal domain (residues 1–101) and the C-terminal domain (residues 135–178) face the cytoplasm. Caveolin-1 undergoes two stages of self-oligomerization. In the first stage, a 41 aa region of the N-terminal domain (residues 61–101) directs the formation of caveolin homo-oligomers [24]. Later, in the second stage, the 44 aa C-terminal domain acts as a bridge to allow these homo-oligomers to interact with each other thereby forming a caveolin-rich scaffold or lattice-work within the plane of the membrane [31].

A number of investigators have purified 'caveolae' from cells and tissues that lack apparent expression of caveolins [32–34]. These membranes were purified based on their Triton insolubility and light buoyant density in sucrose gradients; they have also been purified based simply on their light buoyant density in the absence of detergents. These domains have been termed Triton-insoluble complexes, detergent-resistant membranes, low-density membranes, and caveolae-related domains (CRDs). Like caveolae, these microdomains are dramatically enriched in cholesterol, sphingolipids, and lipid-modified signaling molecules [32,33].

These CRDs can also be produced in vitro simply by mixing cholesterol, sphingolipids, and phospholipids in the appropriate ratio [33]. Their Triton insolubility is apparently a physical property of their molecular organization that produces a liquid-ordered membrane domain (rather than fluid or liquid-crystalline). As caveolin-1 is found associated with glycosphingolipids in vivo as shown using chemical cross-linking with a radio-labeled glycosphingolipid GM_1 [28], binds cholesterol directly [26], and requires a high local concentration of cholesterol ($>30\%$) to insert into model lipid membranes in vitro [26,27], these findings suggest that a true functional relationship exists between CRDs and mature caveolae. For example, during the biogenesis of mature caveolae, CRDs would need to exist as precursors to facilitate the proper insertion of caveolins into membranes. Thus, in cells that express caveolins, these CRDs may represent 'pre-caveolae' that simply lack caveolin proteins. In support of this reductionist model, recombinant expression of caveolin-1 in cells that lack morphologically detectable caveolae is sufficient to drive the formation of mature invaginated caveolae [35–37]. This indicates that cells normally make the ingredients that are necessary for the formation of mature caveolae and insertion of caveolin proteins may be only a late phase in this process. However, it remains unknown whether expression of caveolin-2 or caveolin-3 is sufficient to drive caveolae formation.

Here, we have performed a mutational analysis to determine if specific caveolin-caveolin interactions are required to regulate the size of caveolae, as caveolin-1 undergoes two stages of self-oligomerization. To test this hypothesis directly, we have created two caveolin-1 deletion mutants that lack regions of caveolin-1 that are involved in directing the self-assembly of caveolin-1 oligomers. Our current results show that although these mutants are competent to drive vesicle formation, these vesicles vary widely in their size and shape with diameters up to 500–1000 nm. In addition, we show that caveolin-induced vesicle formation appears to be isoform-specific. Recombinant expression of caveolin-2 under the same conditions failed to drive the formation of vesicles, while caveolin-3 expression yielded caveolae-sized vesicles. As caveolin-2 exists mainly as a monomer or homo-dimer, while caveolins 1 and 3 exist as high molecular mass homo-oligomers, our results are consistent with the idea that the formation of high molecular mass oligomers of caveolin are required to regulate the formation of uniform caveolae-sized vesicles in vivo. This is the first demonstration that the ability to drive the formation of a uniform population of vesicles (50–100 nm in diameter) is unique to caveolins 1 and 3 and requires the ability of caveolin-1 to oligomerize correctly.

2. Materials and methods

2.1. Materials

The cDNAs for caveolins 1, 2 and 3 were as we described previously [4,8,20,22]. Antibodies and their sources were as follows: anti-caveolin-1 (mAb 2297, generous gift of Dr. John R. Glenney, Jr., Transduction Labs); anti-caveolin-2 (mAb 65; Transduction Labs [20]); anti-caveolin-3 (mAb 26; Transduction Labs [21]); and anti-myc (mAb 9E10; Santa Cruz Biotech). The baculovirus expression system was from Clontech: a transfer plasmid vector pBacPAK9 and an engineered baculovirus vector BacPAK6. Normal and Ras-transformed NIH 3T3 cell lines were as we described previously [37,38].

2.2. Insect Sf21 cell culture

Insect *Spodoptera frugiperda* (Sf21) cells were provided by Dr. Takashi Okamoto (Cleveland Clinic Foundation). Sf21 cells were grown in Ex-cell 401 medium containing 10% fetal bovine serum and antibiotics (penicillin-streptomycin) at 27°C.

2.3. Construction of recombinant baculoviruses

cDNAs encoding caveolin-1, caveolin-1 mutants, caveolin-2 and caveolin-3 were subcloned into the multiple cloning site of a transfer plasmid vector, pBacPAK9. A mixture of 2 μg of recombinant plasmid pBacPAK 9 DNA and 1 μg of purified engineered baculoviral vector DNA BacPAK 6 (*Bsu*36I digest) (Clontech) were transfected into insect Sf21 cells, as suggested by the manufacturer [39]. Four days later, culture supernatants were removed and centrifuged at 1000 rpm for 10 min. Clarified supernatants containing wild-type and recombinant baculoviruses were plaque assayed on a monolayer of Sf21 cells. Occlusion negative plaques were picked and seeded onto 2.5×10^6 cells. After 3 days incubation, cells and culture supernatants were removed and centrifuged at 1000 rpm for 10 min. The cell pellets were analyzed by immunoblotting analysis using anti-caveolin antibodies or anti-myc tag mAb 9E10. Those plaques testing positive for the presence of caveolins were selected for three rounds of plaque purification. The selected plaques with highest yield of expression were used as recombinant baculovirus stock for producing protein by infecting insect Sf21 cells.

2.4. Immunoblotting

The expression of caveolins in the baculovirus expression system was evaluated by SDS-PAGE and Western blot analysis. For detection, samples were separated using SDS-PAGE (10% or 15% acrylamide) and transferred to nitrocellulose for primary antibody binding (anti-caveolin antibodies or anti-myc mAb 9E10). HRP-conjugated secondary antibodies (1:5000 dilution, Amersham) were used to visualize bound primary antibodies by an enhanced chemiluminescence assay (ECL; Amersham).

2.5. Electron microscopy

Transmission electron microscopy was performed as described previously by our laboratory. Samples were fixed with glutaraldehyde, postfixed with osmium tetroxide, and stained with uranyl acetate and lead citrate, as detailed in [8,10]. Samples were examined under the Philips 410 TEM.

2.6. Triton insolubility

The Triton solubility of a given protein was determined essentially as we described previously, with minor modifications [9]. Briefly, NIH 3T3 cells grown to confluence in 35 mm dishes were first extracted with 1 ml of MES-buffered saline (MBS, 25 mM MES, pH 6.5, 0.15 M NaCl) containing 1% Triton X-100 and 1 mM PMSF. After 30 min on ice without agitation, the Triton-soluble extract (S) was gently decanted and the remaining Triton-insoluble material (I) was solubi-

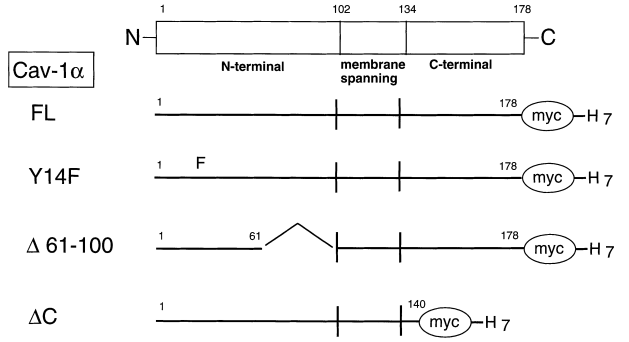

Fig. 1. Construction of caveolin-1 mutants for expression in Sf21 insect cells. Full-length caveolin-1 (FL), a tyrosine-to-phenylalanine point mutant (Y14F), an internal deletion mutant lacking the oligomerization domain (Δ61–100), and a mutant lacking a complete C-terminal domain (ΔC) are shown. Note that all constructs contain a C-terminal myc tag, followed by a polyhistidine tag.

lized in 1 ml of 1% SDS. Each extract was then concentrated by acetone precipitation, solubilized in 10% SDS, and diluted into 4× sample buffer for analysis by SDS-PAGE and Western blotting.

2.7. Cell fractionation

NIH 3T3 cells were grown to confluence in 150 mm dishes and used to prepare caveolin-enriched membrane fractions, essentially as described [3,8,10,40]. Briefly, NIH 3T3 cells from a confluent 150 mm dish were scraped into 2 ml of MBS containing 1% Triton X-100 and 1 mM PMSF. Homogenization was carried out with 10 strokes of a loose-fitting Dounce homogenizer. The homogenate was adjusted to 40% sucrose by addition of 2 ml of 80% sucrose prepared in MBS and placed at the bottom of an ultracentrifuge tube. A 5–30% linear sucrose gradient was formed above the homogenate and centrifuged at 39 000 rpm for 16–20 h in a SW41 rotor (Beckman Instruments, Palo Alto, CA). A light-scattering band confined to the 15–20% sucrose region is harvested, diluted 3-fold with MBS and pelleted in the microfuge (14 000×*g*; 15 min at 4°C). The majority of protein remained within the 40% sucrose region of the gradient. Approximately 4–6 μg of caveolin-enriched domains were obtained from one 150 mm dish of cells representing 10 mg of protein, a yield of ∼0.05% relative to the homogenate. We and other laboratories have demonstrated that these domains exclude a variety of organelle-specific membrane markers (for ER, Golgi, lysosomes, mitochondria and non-caveolar plasma membrane), but are dramatically enriched ∼2000-fold in caveolin-1, a caveolar marker protein [3,8,10,13,40,41].

3. Results

3.1. Baculovirus-based expression of wild-type caveolin-1 and caveolin-1 mutants in Sf21 insect cells

Full-length caveolin-1 or a variety of caveolin-1 mutants (Y14F, Δ61–100, and ΔC) were integrated into an engineered baculovirus genome via a recombinant transfer plasmid, as detailed in Section 2. For these constructions, a myc epitope tag was placed at the C terminus with a polyhistidine tag following the myc tag (Fig. 1).

Wild-type caveolin-1 and caveolin-1 mutants were all expressed very well in Sf21 insect cells using the baculovirus system. Fig. 2A shows that wild-type caveolin-1 and caveolin-1 mutants migrated at their expected molecular weight, including the myc and polyhistidine tags. We and others have previously shown that these tags do not interfere with the targeting of recombinant caveolins or the ability of caveolin-1 expression to drive vesicle formation [4,19,22,36,42–45]. In addition, expression of caveolin-1 in insect cells using the baculovirus system allowed the expression of ∼50–100-fold more caveolin-1 protein, as compared with a mammalian cell line (NIH 3T3) that normally expresses caveolin-1 (Fig. 2B).

Electron microscopic analysis of uninfected Sf21 insect cells did not show the appearance of caveolae, as we have reported previously [36] (Fig. 3A). However, insect cells infected with wild-type full length caveolin-1 accumulated a uniform population of caveolae-like structures within their cytoplasm. This

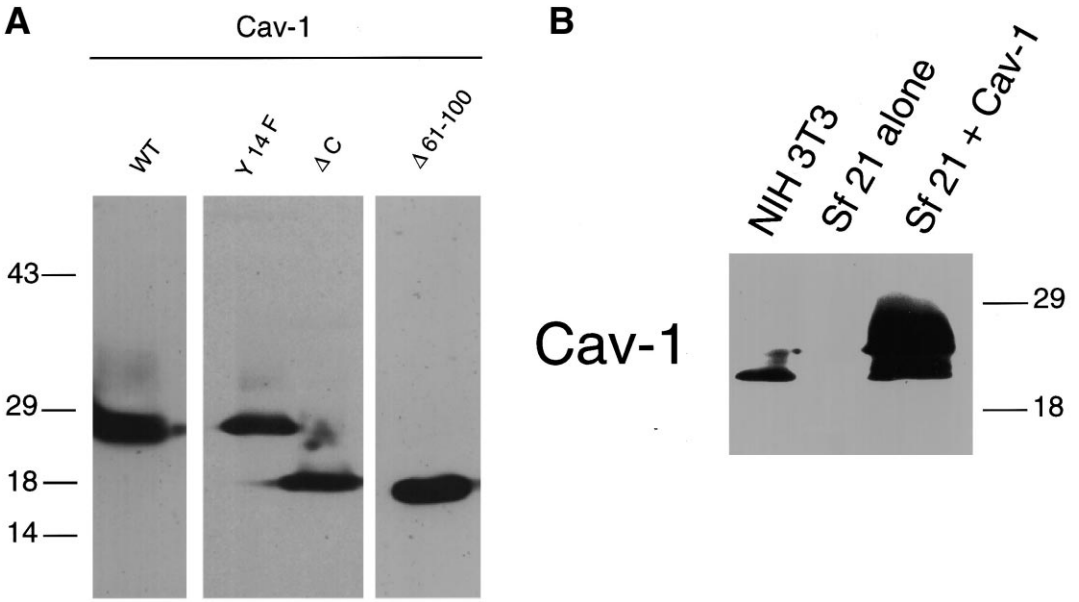

Fig. 2. Expression of full-length caveolin-1 and caveolin-1 mutants in Sf21 insect cells. A: Lysates from insect cells infected with a given baculovirus vector were prepared and subjected to immunoblot analysis with a monoclonal antibody probe that recognizes the myc epitope (mAb 9E10). B: Lysates from NIH 3T3 cells and insect cells expressing caveolin-1 were compared by Western blot analysis using a caveolin-1-specific monoclonal antibody probe (2297). Note that expression of caveolin-1 in insect cells using the baculovirus system allowed the expression of ∼50–100-fold more caveolin-1 protein, as compared with a mammalian cell line (NIH 3T3 cells). Uninfected Sf21 cells served as a negative control. Each lane contains equal amounts of total protein.

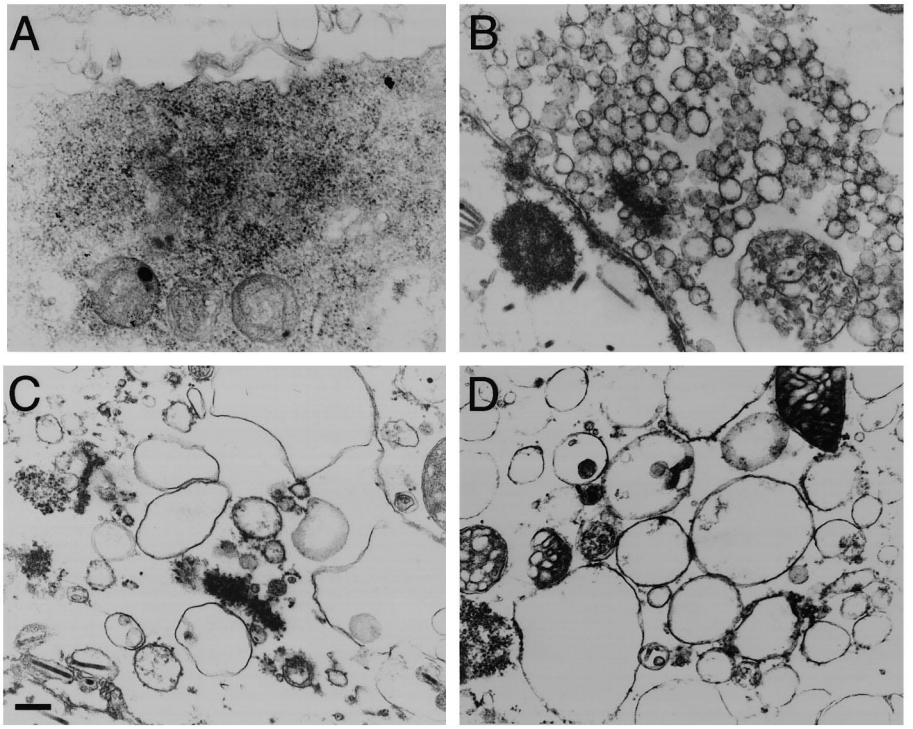

Fig. 3. Morphological analysis of caveolin-induced vesicle formation. Sf21 insect cells were infected with either full-length caveolin-1 or a given caveolin-1 mutant. Cells were fixed and processed for transmission electron microscopy. A: Uninfected control cells lacking caveolin-1 induced vesicles. B: Infected Sf21 cells expressing caveolin-1 FL contain a uniform population of caveolin-1-induced vesicles of ~50–100 nm in diameter. C: Infected Sf21 cells expressing caveolin-1 (Δ61–100). D: Infected Sf21 cells expressing caveolin-1 (ΔC). Note that in panels C and D, caveolin-1-induced vesicles were produced, but they have a much larger diameter and are irregular in size and shape. Bar = 100 nm.

population of vesicles was homogeneous in size and is the same size as expected for mammalian caveolae, ~50–100 nm in diameter (Fig. 3B). Virtually identical results were observed with caveolin-1 Y14F, indicating that tyrosine phosphorylation of this residue is not required for caveolin-1-induced vesicle formation (not shown). Src tyrosine kinases are known to phosphorylate caveolin-1 on tyrosine 14 both in vitro and in vivo [46].

Both caveolin-1 mutants, Δ61–100, and ΔC, also retained the ability to drive vesicle formation (Fig. 3C,D). However, these vesicles varied widely in their size and shape with diameters up to 500–1000 nm. As these two mutants lack specific regions of caveolin-1 that have been implicated in caveolin-1 oligomerization, it appears that these caveolin-caveolin interactions may be necessary to regulate the uniform 50–100 nm diameter that is characteristic of caveolae in vivo.

3.2. Caveolin-induced vesicle formation is isoform-specific: expression of caveolin-2 does not drive vesicle formation

As previous reports have only examined the ability of caveolin-1 to drive the formation of caveolae and caveolin-induced vesicles, we next assessed the ability of caveolin-2 and caveolin-3 to drive vesicle formation. Caveolins 1 and 2 are usually co-expressed and demonstrate the same tissue distribution [4,20]; in contrast, the expression of caveolin-3 is confined to muscle cell types (smooth, cardiac and skeletal) [21–23]. Interestingly, caveolins 1 and 3 assemble into high molecular mass homo-oligomers of ~350 kDa [22,24]. On the other hand, caveolin-2 primarily exists as a monomer or dimer and requires caveolin-1 co-expression to assemble into a high molecular mass complex of ~350 kDa [4,20].

Caveolins 1, 2, and 3 were all equally well expressed in Sf21 insect cells infected with a given baculovirus (Fig. 4). Electron microscopic analysis revealed that cells infected with either caveolin-1 or caveolin-3 accumulated a uniform population

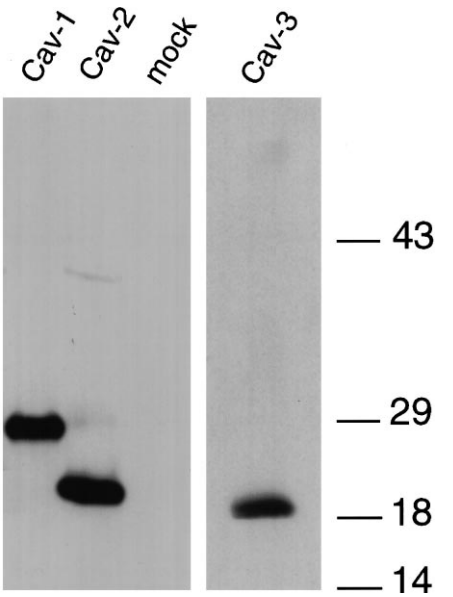

Fig. 4. Expression of full-length caveolins 1, 2 and 3 in Sf21 insect cells. Lysates from insect cells infected with a given baculovirus vector were prepared and subjected to immunoblot analysis with a monoclonal antibody probe that recognizes the myc epitope (mAb 9E10). Note that all three caveolins were equally well expressed using this approach.

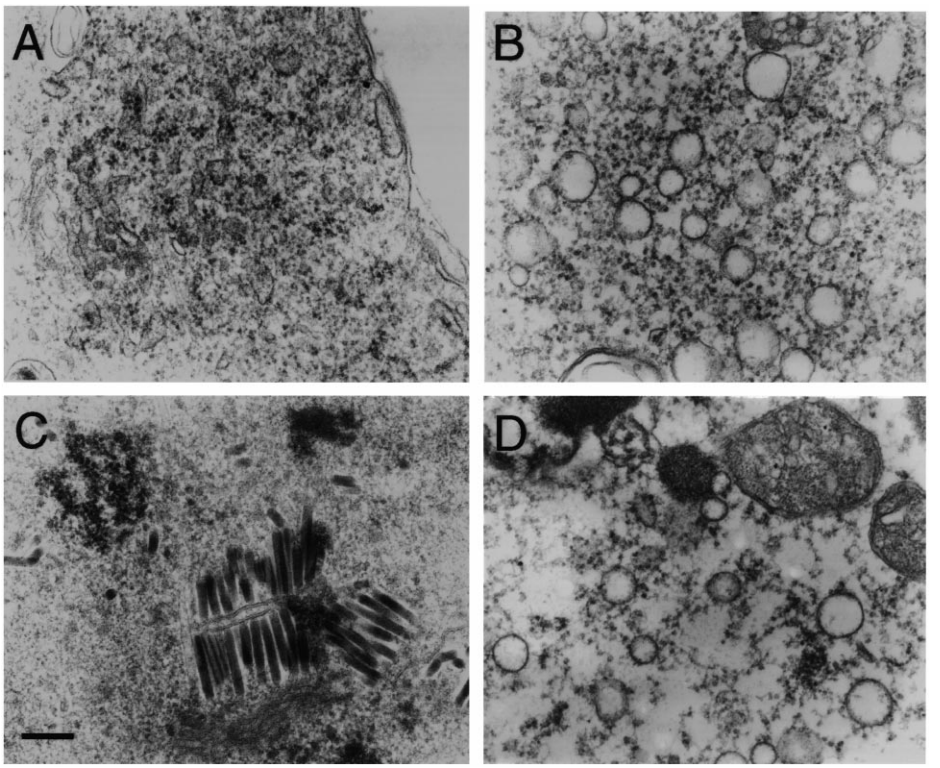

Fig. 5. Expression of caveolin-2 fails to drive caveolin-induced vesicle formation in Sf21 insect cells. A: Uninfected control cells. B: Cells infected with caveolin-1. C: Cells infected with caveolin-2. D: Cells infected with caveolin-3. Note that expression of caveolins 1 and 3 (panels B and D) is sufficient to drive the formation of a uniform population of caveolin-induced vesicles with a diameter of 50–100 nm. In contrast, expression of caveolin-2 (panel C) does not drive vesicle formation, despite evidence of infection such as viral particles (which appear as short and long black bar-like structures). Bar = 100 nm.

of caveolae-like structures within their cytoplasm (Fig. 5). This population of vesicles was homogeneous in size, with a diameter of ~50–100 nm. In contrast, expression of caveolin-2 did not drive vesicle formation, despite evidence of infection such as viral particles (Fig. 5). These results indicate that a transmembrane domain alone is not sufficient to drive vesicle formation in Sf21 insect cells.

Co-infection of insect cells with baculoviruses encoding caveolins 1 and 2 also resulted in the formation of a uniform population of caveolae-like structures. However, these vesicles appeared smaller in size, with a diameter of ~45–65 nm (Fig. 6). These results indicate that interactions between caveolins 1 and 2 can also serve to regulate the diameter of caveolae-like vesicles.

3.3. Caveolin-1 recruits caveolin-2 to caveolae membranes

NIH 3T3 cells co-express caveolins 1 and 2 where they form a stable hetero-oligomeric complex in vivo and both are targeted to caveolae membranes [20]. However, in NIH 3T3 cells transformed by activated oncogenes, such as activated Ras (G12V), caveolin-1 mRNA and protein expression are selectively down-regulated [37]. Under these conditions, caveolin-2 protein levels remain relatively constant [20]. Thus, we compared the properties of caveolin-2 in normal and Ras-transformed NIH 3T3 cells to assess the effects of caveolin-1 down-regulation on the behavior and localization of caveolin-2.

There are now three recognized isoforms of caveolin-2 (α, β, and γ). Cav-2α and Cav-2β are thought to be generated by from a single mRNA species using alternative translation initiation sites (M1 and M13), while the origin and primary sequence of Cav-2γ remains unknown ([20]; and unpublished observations). Interestingly, Cav-2γ is abundantly expressed in astrocytes (data not shown).

Fig. 7A shows that loss of caveolin-1 expression in Ras-transformed NIH 3T3 cells results in the selective down-regulation of both Cav-2β and Cav-2γ isoforms, while the levels of Cav-2α remain relatively constant. In addition, in the ab-

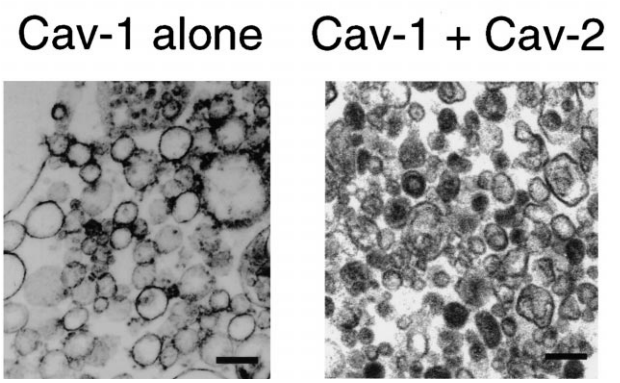

Fig. 6. Caveolae-like vesicles are smaller in cells co-infected with caveolin-1 and caveolin-2. Co-infection of insect cells with baculoviruses encoding caveolins 1 and 2 also resulted in the formation of a uniform population of caveolae-like structures. However, these vesicles appeared smaller in size, with a diameter of ~45–65 nm. These results indicate that interactions between caveolins 1 and 2 can also serve to regulate the diameter of caveolae-like vesicles. Left panel, caveolin-1 alone; right panel, caveolin-1 plus caveolin-2. Bar = 100 nm.

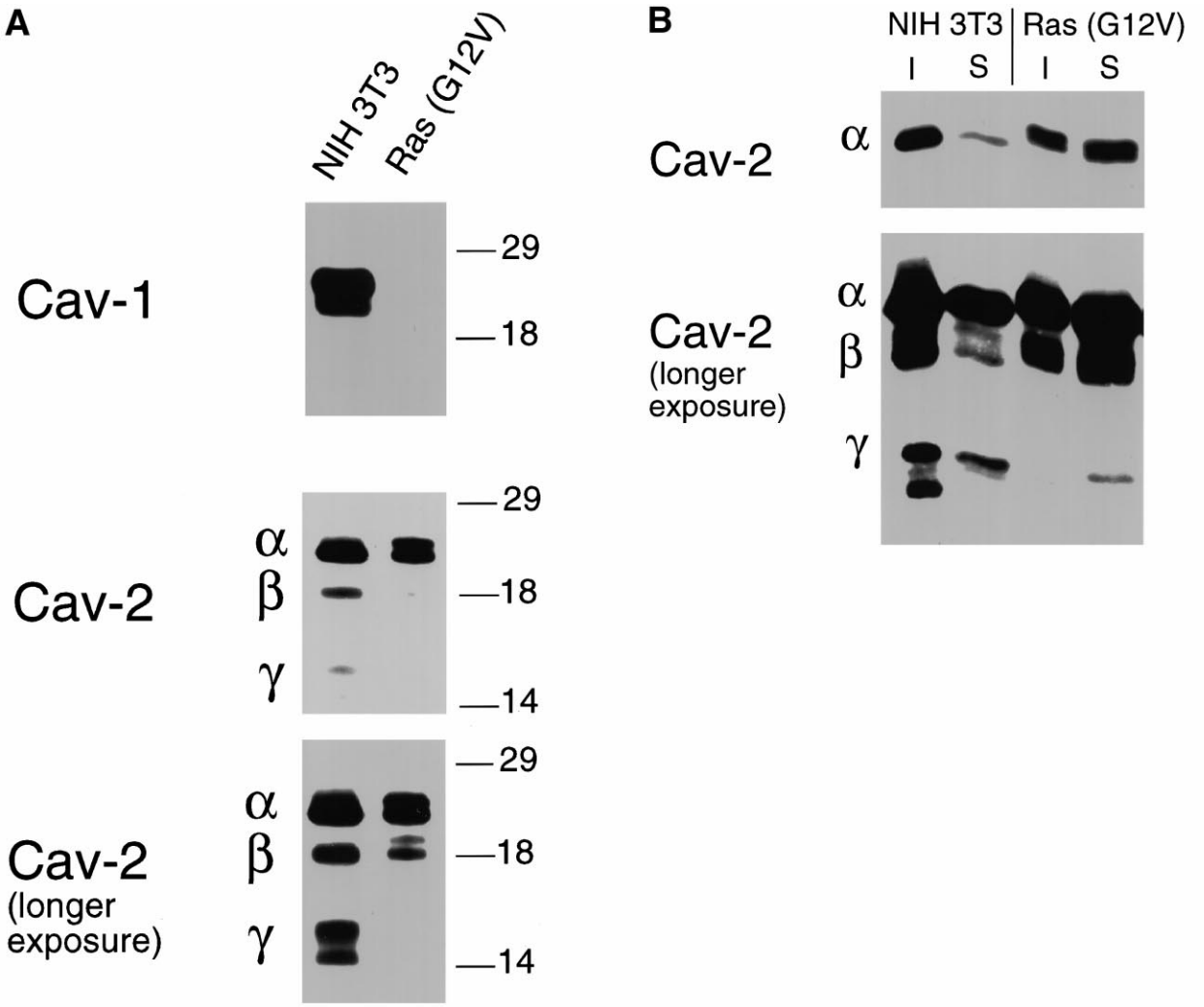

Fig. 7. Down-regulation of caveolin-1 affects the expression and detergent insolubility of caveolin-2 isoforms. A: Expression of caveolin-1 and caveolin-2 isoforms (α, β, and γ) in normal and Ras-transformed NIH 3T3 cells. B: Detergent insolubility of caveolin-2 isoforms (α, β, and γ) in normal and Ras-transformed NIH 3T3 cells. I, Triton-insoluble; S, Triton-soluble. Each lane contains equal amounts of total protein. Caveolins 1 and 2 were detected by Western blot analysis using mono-specific antibody probes: anti-caveolin-1 IgG (mAb 2297) and anti-caveolin-2 (mAb 65). In A and B, multiple exposures are shown to illustrate the different isoforms of caveolin-2. Note that Cav-2β is much less abundant than Cav-2α and Cav-2γ is the least abundant isoform.

sence of caveolin-1 expression, all three caveolin-2 isoforms appeared to become predominantly Triton-soluble (~60–100%), while all three caveolin-2 isoforms were >90% Triton-insoluble in normal NIH 3T3 cells which express caveolin-1 (Fig. 7B). These results suggest that the stability and Triton-insolubility of caveolin-2 isoforms may be dependent on co-expression with caveolin-1. As caveolae and CRDs are Triton-insoluble membrane compartments [3,8–13], these results also suggest that caveolin-2 requires caveolin-1 to localize to these cholesterol/sphingolipid-rich microdomains.

To test this hypothesis directly, we next utilized a Ras-transformed NIH 3T3 cell line that harbors caveolin-1 under the control of an inducible promoter. In this previously characterized cell line, recombinant caveolin-1 can be induced by addition of the simple sugar IPTG to the culture medium [37].

We analyzed the distribution of caveolin-1 and -2 in this cell line using an established biochemical procedure that separates caveolae and CRDs from the bulk of cellular membranes and cytosolic proteins [3,8,10,13,40,41,43,47–50]. In this fractionation scheme, immunoblotting with anti-caveolin-1 IgG can be used to track the position of caveolae-derived membranes within these bottom-loaded sucrose gradients. Using this procedure, caveolin-1 is purified ~2000-fold relative to total cell lysates as ~4–6 μg of caveolin-rich domains (containing ~90–95% of total cellular caveolin-1) are obtained from 10 mg of total cellular proteins [41,48]. We and others have shown that these caveolin-rich fractions exclude >99.95% of total cellular proteins and also markers for non-caveolar plasma membrane, Golgi, lysosomes, mitochondria and endoplasmic reticulum [3,8,10].

Fig. 8A shows that recombinant caveolin-1 was correctly targeted to caveolae membranes (fractions 4 and 5) after inducing its expression by incubation with IPTG. Interestingly, in the absence of caveolin-1 induction, only ~40–50% of Cav-2α was targeted to caveolae membranes, while Cav-2β was completely excluded from caveolae membranes and Cav-2γ was undetectable. In contrast, after induction of caveolin-1 expression, all three caveolin-2 isoforms were predominantly localized to caveolae and Cav-2β and Cav-2γ were upregulated (Fig. 8B). As caveolins 1 and 2 are known to

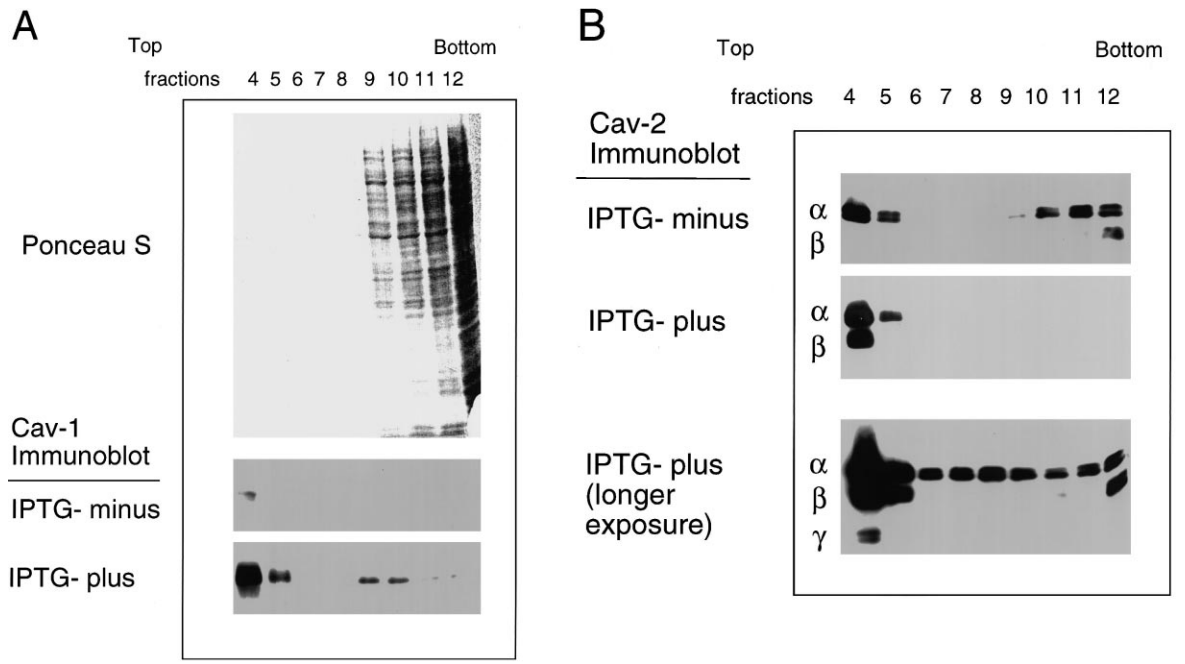

Fig. 8. Induction of caveolin-1 expression recruits caveolin-2 isoforms to caveolae membranes. A: Distribution of total cellular proteins (visualized by Ponceau S staining) and caveolin-1. Note that recombinant caveolin-1 was correctly targeted to caveolae membranes (fractions 4 and 5) after inducing its expression by incubation with IPTG. B: Distribution of caveolin-2 isoforms (α, β, and γ) before and after induction of the expression of recombinant caveolin-1 using IPTG. Note that in the absence of caveolin-1 induction, only ~40–50% Cav-2α was targeted to caveolae membranes (fractions 4 and 5), while Cav-2β was completely excluded from caveolae membranes and Cav-2γ was undetectable. In contrast, after induction of caveolin-1 expression, all three caveolin-2 isoforms were predominantly localized to caveolae (fractions 4 and 5) and Cav-2β and Cav-2γ were upregulated. Caveolins 1 and 2 were detected by Western blot analysis using mono-specific antibody probes: anti-caveolin-1 IgG (mAb 2297) and anti-caveolin-2 (mAb 65). In panel B, multiple exposures are shown to illustrate the different isoforms of caveolin-2. Fractions 1–3 have been omitted as they do not contain any protein or caveolin isoforms, as we and others have indicated in previous reports [3,8,10,13,40,41].

form a large hetero-oligomeric complex in vivo [20,24], our results clearly indicate that caveolin-1 expression stabilizes and recruits caveolin-2 isoforms to caveolae membranes.

These results are also consistent with our morphological observations in insect cells: (i) that caveolin-2 expression alone is not sufficient to generate caveolae-like vesicles; and (ii) that co-expression of caveolins 1 and 2 in insect cells yields the formation of caveolae-like vesicles that are of a smaller diameter than those generated using caveolin-1 alone. Taken together, these observations suggest that caveolin-2 may function as an 'accessory protein' in conjunction with caveolin-1.

4. Discussion

We have previously developed a functional assay system to monitor the ability of caveolin-1 expression to drive the formation of a uniform population of caveolae-sized vesicles [36]. In this system, Sf21 insect cells were infected with a baculovirus vector encoding caveolin-1α (residues 1–178) or caveolin-1β (residues 32–178) and examined by transmission electron microscopy. Results of these studies indicated that recombinant expression of caveolin-1 is sufficient to drive vesicle formation and that residues 1–32 of caveolin-1 are not required for this process [36]. As cholesterol and sphingolipids are important lipid components of caveolae membranes in mammalian cells, it is important to note that insect cells also use sphingolipids and plasma membrane sterols, including cholesterol [51,52].

Here, we have employed this morphological assay system to perform a mutational analysis of the ability of caveolin-1 to drive the formation of caveolae-sized vesicles. We have shown that caveolin-1 deletion mutants (Δ61–100 and ΔC), lacking either the N-terminal oligomerization domain or the extreme C-terminal domain, are sufficient to drive vesicle formation. However, these vesicles are larger and appear irregular in their size and shape. Additionally, we show that while caveolins 1 and 3 are competent to drive vesicle formation, caveolin-2 expression fails to drive the formation of any vesicles (regular or irregular). Thus, the ability to drive the formation of a uniform population of vesicles (50–100 nm in diameter) is unique to caveolins 1 and 3 and requires the ability of caveolin-1 to oligomerize correctly.

As caveolin-2 fails to drive vesicle formation, this should be extremely useful in future mutational studies aimed at determining which regions of caveolin-1 are sufficient to allow caveolin-2 to drive vesicle formation. For example, such a study could be carried out by constructing a panel of chimeric proteins containing regions of both caveolin-1 and caveolin-2.

Recently, we have reported that the co-expression of caveolins 1 and 2 is uncoupled by cellular transformation by activated oncogenes, such as v-Abl and activated H-Ras (G12V). While caveolin-1 mRNA and protein levels are down-regulated in response to cellular transformation [38], caveolin-2 protein levels remain relatively unchanged [20]. While these cells continue to express caveolin-2 protein, they fail to contain detectable caveolae, as we have reported previously [38]. These observations suggest that caveolin-2 ex-

pression alone is not sufficient to drive the formation of morphologically detectable caveolae.

In support of this idea, we show here that expression of caveolin-2 in Sf21 insects cells fails to drive the formation of caveolae-like vesicles, while recombinant expression of caveolin-1 within the same cell system is sufficient to drive the formation of hundreds of uniform caveolae-like vesicles (50–100 nm in diameter). In addition, we demonstrate that: (i) coexpression of caveolins 1 and 2 in insect cells yields the formation of caveolae-like vesicles that are of a smaller diameter than those generated using caveolin-1 alone; and (ii) caveolin-1 expression in mammalian cells stabilizes and recruits caveolin-2 isoforms to caveolae membranes. Our results are consistent with the idea that caveolin-2 expression alone is not sufficient to drive caveolae formation and that caveolin-2 may function as an 'accessory protein' in conjunction with caveolin-1.

Acknowledgements: We thank members of the Lisanti laboratory for helpful and insightful discussions, Ya-Huei Tu for electron microscopic analysis and Drs. John R. Glenney and Roberto Campos-Gonzalez (Transduction Laboratories) for donating anti-caveolin mAb probes. This work was supported by an NIH FIRST Award GM-50443 (to M.P.L.), and grants from the Charles E. Culpeper Foundation (to M.P.L.), G. Harold and Leila Y. Mathers Charitable Foundation (to M.P.L. and P.E.S.) and the Sidney Kimmel Foundation for Cancer Research (to M.P.L.). P.E.S. was supported by a grant from Pfizer Corp., a pilot grant from the AECOM DRTC, and by a research grant from the American Diabetes Association. S.L. is the recipient of an NIH-NCI Post-doctoral Fellowship, CA-71326.

References

[1] Severs, N.J. (1988) J. Cell Sci. 90, 341–348.
[2] Fan, J.Y., Carpentier, J.-L., van Obberghen, E., Grunfeld, C., Gorden, P. and Orci, L. (1983) J. Cell Sci. 61, 219–230.
[3] Scherer, P.E., Lisanti, M.P., Baldini, G., Sargiacomo, M., Corley-Mastick, C. and Lodish, H.F. (1994) J. Cell Biol. 127, 1233–1243.
[4] Scherer, P.E., Okamoto, T., Chun, M., Nishimoto, I., Lodish, H.F. and Lisanti, M.P. (1996) Proc. Natl. Acad. Sci. USA 93, 131–135.
[5] Simionescu, N. and Simionsecu, M. (1983) in: Histology: Cell and Tissue Biology (Weiss, L., Ed.), pp. 371–433, Elsevier Biomedical, New York.
[6] Forbes, M.S., Rennels, M. and Nelson, E. (1979) J. Ultrastruct. Res. 67, 325–339.
[7] Bretscher, M. and Whytock, S. (1977) J. Ultrastruct. Res. 61, 215–217.
[8] Sargiacomo, M., Sudol, M., Tang, Z.-L. and Lisanti, M.P. (1993) J. Cell Biol. 122, 789–807.
[9] Lisanti, M.P., Tang, Z.-L. and Sargiacomo, M. (1993) J. Cell Biol. 123, 595–604.
[10] Lisanti, M.P., Scherer, P.E., Vidugiriene, J., Tang, Z.-L., Hermanoski-Vosatka, A., Tu, Y.-H., Cook, R.F. and Sargiacomo, M. (1994) J. Cell Biol. 126, 111–126.
[11] Chang, W.J. et al. (1994) J. Cell Biol. 126, 127–138.
[12] Schroeder, R., London, E. and Brown, D. (1994) Proc. Natl. Acad. Sci. USA 91, 12130–12134.
[13] Schnitzer, J.E., Oh, P., Jacobson, B.S. and Dvorak, A.M. (1995) Proc. Natl. Acad. Sci. USA 92, 1759–1763.
[14] Moldovan, N., Heltianu, C., Simionescu, N. and Simionescu, M. (1995) Exp. Cell Res. 219, 309–313.
[15] Glenney, J.R. (1989) J. Biol. Chem. 264, 20163–20166.
[16] Glenney, J.R. and Soppet, D. (1992) Proc. Natl. Acad. Sci. USA 89, 10517–10521.
[17] Glenney, J.R. (1992) FEBS Lett. 314, 45–48.
[18] Rothberg, K.G., Heuser, J.E., Donzell, W.C., Ying, Y., Glenney, J.R. and Anderson, R.G.W. (1992) Cell 68, 673–682.
[19] Kurzchalia, T., Dupree, P., Parton, R.G., Kellner, R., Virta, H., Lehnert, M. and Simons, K. (1992) J. Cell Biol. 118, 1003–1014.
[20] Scherer, P.E. et al. (1997) J. Biol. Chem. 272, 29337–29346.
[21] Song, K.S. et al. (1996) J. Biol. Chem. 271, 15160–15165.
[22] Tang, Z.-L. et al. (1996) J. Biol. Chem. 271, 2255–2261.
[23] Way, M. and Parton, R. (1995) FEBS Lett. 376, 108–112.
[24] Sargiacomo, M., Scherer, P.E., Tang, Z.-L., Kubler, E., Song, K.S., Sanders, M.C. and Lisanti, M.P. (1995) Proc. Natl. Acad. Sci. USA 92, 9407–9411.
[25] Monier, S., Parton, R.G., Vogel, F., Behlke, J., Henske, A. and Kurzchalia, T. (1995) Mol. Biol. Cell 6, 911–927.
[26] Murata, M., Peranen, J., Schreiner, R., Weiland, F., Kurzchalia, T. and Simons, K. (1995) Proc. Natl. Acad. Sci. USA 92, 10339–10343.
[27] Li, S., Song, K.S. and Lisanti, M.P. (1996) J. Biol. Chem. 271, 568–573.
[28] Fra, A.M., Masserini, M., Palestini, P., Sonnino, S. and Simons, K. (1995) FEBS Lett. 375, 11–14.
[29] Couet, J., Li, S., Okamoto, T., Scherer, P.S. and Lisanti, M.P. (1997) Trends Cardiovasc. Med. 7, 103–110.
[30] Okamoto, T., Schlegel, A., Scherer, P.E. and Lisanti, M.P. (1998) J. Biol. Chem. 273, 5419–5422.
[31] Song, K.S., Tang, Z.-L., Li, S. and Lisanti, M.P. (1997) J. Biol. Chem. 272, 4398–4403.
[32] Simons, K. and Ikonen, E. (1997) Nature 387, 569–572.
[33] Brown, D.A. and London, E. (1997) Biochem. Biophys. Res. Commun. 240, 1–7.
[34] Kubler, E., Dohlman, H.G. and Lisanti, M.P. (1996) J. Biol. Chem. 271, 32975–32980.
[35] Fra, A.M., Williamson, E., Simons, K. and Parton, R.G. (1995) Proc. Natl. Acad. Sci. USA 92, 8655–8659.
[36] Li, S., Song, K.S., Koh, S., Kikuchi, A. and Lisanti, M.P. (1996) J. Biol. Chem. 271, 28647–28654.
[37] Engelman, J.A., Wycoff, C.C., Yasuhara, S., Song, K.S., Okamoto, T. and Lisanti, M.P. (1997) J. Biol. Chem. 272, 16374–16381.
[38] Koleske, A.J., Baltimore, D. and Lisanti, M.P. (1995) Proc. Natl. Acad. Sci. USA 92, 1381–1385.
[39] Summers, M.D. and Smith, G.E. (1987) Texas Agric. Exp. Stn. Bull., no. 1555.
[40] Smart, E., Ying, Y.-S., Conrad, P. and Anderson, R.G.W. (1994) J. Cell Biol. 127, 1185–1197.
[41] Lisanti, M.P., Tang, Z.-T., Scherer, P. and Sargiacomo, M. (1995) Methods Enzymol. 250, 655–668.
[42] Dietzen, D.J., Hastings, W.R. and Lublin, D.M. (1995) J. Biol. Chem. 270, 6838–6842.
[43] Scherer, P.E., Tang, Z.-L., Chun, M.C., Sargiacomo, M., Lodish, H.F. and Lisanti, M.P. (1995) J. Biol. Chem. 270, 16395–16401.
[44] Song, K.S., Li, S., Okamoto, T., Quilliam, L., Sargiacomo, M. and Lisanti, M.P. (1996) J. Biol. Chem. 271, 9690–9697.
[45] Tang, Z., Okamoto, T., Boontrakulpoontawee, P., Katada, T., Otsuka, A.J. and Lisanti, M.P. (1997) J. Biol. Chem. 272, 2437–2445.
[46] Li, S., Seitz, R. and Lisanti, M.P. (1996) J. Biol. Chem. 271, 3863–3868.
[47] Sargiacomo, M., Scherer, P.E., Tang, Z.-L., Casanova, J.E. and Lisanti, M.P. (1994) Oncogene 9, 2589–2595.
[48] Li, S., Okamoto, T., Chun, M., Sargiacomo, M., Casanova, J.E., Hansen, S.H., Nishimoto, I. and Lisanti, M.P. (1995) J. Biol. Chem. 270, 15693–15701.
[49] Corley-Mastick, C., Brady, M.J. and Saltiel, A.R. (1995) J. Cell Biol. 129, 1523–1531.
[50] Robbins, S.M., Quintrell, N.A. and Bishop, M.J. (1995) Mol. Cell. Biol. 15, 3507–3515.
[51] Gimpl, G., Klein, U., Reilander, H. and Fahrenholz, F. (1995) Biochemistry 34, 13794–13801.
[52] Wiegandt, H. (1992) Biochim. Biophys. Acta 1123, 117–126.